

Mode conversion of elastic waves by using anisotropic metamaterials

Xiongwei YANG; Yueming LI; Gang Chen

State Key Laboratory for Strength and Vibration of Mechanical Structures, School of Aerospace, Xi'an Jiaotong University, No.28 Xianning West Road, 710049 Xi'an, China

ABSTRACT

As a fundamental phenomenon in elastic fields, mode conversion between longitudinal and transverse wave modes can frequently occur when a wave is incident on an elastic discontinuity or passes through anisotropic mediums. Due to the generation of a different wave mode, the phenomenon is widely used in industrial and medical applications for nondestructive tests and ultrasonic inspections. Metamaterials are man-made subwavelength composites and could be designed based on the local resonance mechanism. Due to local resonance, effective physical properties of the metamaterials could be zero or negative in desired frequency ranges, leading to novel wave phenomena, such as low frequency bandgap. Metamaterials could also be designed with specific macroscopic anisotropy in specific direction. Such anisotropic metamaterials, if designed to be nonresonant, barely exhibit material absorption losses, and could be more suitable for wave manipulating, such as acoustic magnifying, invisibility cloaking. In this work, we are concerned whether the resonance mechanism can be introduced into mode conversion. Because of the resonance mechanism, the effective properties of the metamaterials can be highly frequency-dependent, which means vast possibilities in finding new phenomena and obtaining new designs. Our final goal is to pave the way of using the frequency-dependency concept for mode conversion.

Keywords: Elastic wave, Mode conversion, Anisotropic metamaterial

1. INTRODUCTION

The phenomenon of mode conversion between different wave modes can be frequently noticed in elastic fields, such as when an elastic wave is incident on an elastic discontinuity or passes through anisotropic mediums. Because the wave mode defines the fundamental characteristics of how wave energy propagates, changing of the wave mode, i.e., realization of mode conversion, could be of great scientific importance and engineering significance^[1-3]. For example, shear (transverse) waves, which are difficult to generate, can be critically useful in structural non-destructive evaluation and medical imaging, because of their sensitivity to elastic discontinuities or biomedical focuses. On the other hand, longitudinal waves, are much easier in generation, yet less sensitive to elastic discontinuities or biomedical focuses. Therefore, mode-conversion from longitudinal waves could be a potential way for the efficient generation of transverse waves. In non-destructive evaluation, wedge-type mode convertors, which work according to the Snell's law, are commonly used^[4]. However, due the inevitable generation of longitudinal wave mode, the mode-converting efficiency is rather low, normally about 25%. Researchers then noticed that if double- or triple- negative metamaterials are used to design the wedge-type mode convertors, complete mode-converting transmission could be theoretically possible, but requires that some additional conditions must be fulfilled between the background test medium and the mode convertors^[5-7]. Because the conditions are too restrictive, so far, no realization of complete mode-converting transmission has been attempted with double or triple negative metamaterials. The mode-converting efficiency, is about 40%. Additionally, because of the high frequency-dependency of the effective material properties, the frequency range with a relatively higher mode-converting efficiency could be rather narrow.

Recently, perfect transmodal Fabry-perot interference^[8-9] allows a sole and maximal mode conversion between longitudinal and transverse wave modes. In such a phenomenon, under incidence of a longitudinal wave mode, there is only the transmission of the transverse wave. Because of the multimodal constructive interference, the displacement amplitudes before and after transmission are the same. However, same displacement amplitudes indicate different energy, because the

longitudinal and transverse wave modes are determined by different stiffness coefficients. Even in the same isotropic media, the transverse stiffness coefficient differs from the longitudinal stiffness coefficient. Therefore, complete mode-converting transmission is only possible, when elastic waves propagate in the same background media which has the same transverse and longitudinal stiffness coefficients. Since the impedance mismatch is the reason that complete mode-converting transmission cannot be accomplished in the perfect transmodal Fabry-perot interference, a bimodal quarter-wave impedance matching theory^[10] was thereafter developed, which seeks complete mode-converting transmission through matching impedances of the incident longitudinal wave mode and the transmitted transverse wave mode. Because the impedances can be matched regardless of the background media, complete mode-converting transmission between longitudinal and transverse wave modes can be realized not only in the same background medium, but also between different media.

Realization of the theories, either the perfect transmodal Fabry-perot interference theory or the bimodal quarter-wave impedance matching theory, requires that the interferometer or the matching element must have very specific anisotropy. Therefore, anisotropic metamaterials were designed for the realization of the unique material properties. However, because the anisotropic metamaterials were designed to be nonresonant, their dimensions must be much smaller than the wavelength. This means that, if designed in the ultrasonic frequency range, unit cell of the metamaterials could be too small to fabricate, while if designed in the low frequency range, unit cell could be too larger to fabricate. Therefore, in this work, we seek to introduce resonance into the design of anisotropic metamaterials. This is possible, because the resonance mechanism can induce extraordinary effective material properties for unusual wave phenomenon.

2. THEORY

Consider an elastic wave which is propagating in a two-dimensional x - y plane through an anisotropic elastic slab (with width d), which is sandwiched between layers of another base medium. Here, we mainly consider a propagating longitudinal wave, which is normally incident from the base medium to the anisotropic slab.

2.1 Theoretical background

For the analysis considerer here, the stiffness coefficients needed are C_{11} , C_{66} , and C_{16} for the slab medium. The stiffness terms with subscripts (11) and (66) denote the longitudinal stiffness along the x axis and the shear stiffness, respectively, while the term with (16) refers to the longitudinal-shear coupling term. For common cases, we consider that the base medium is isotropic, which will be characterized by Young's modulus (E_0) and Poisson's ratio (ν_0). The symbols ρ_0 and ρ will be used to denote the densities of the base material and slab material, respectively.

For waves propagating along the x direction, the x - and y -directional displacements u_x and u_y can be assumed to vary as $e^{j(kx - \omega t)}$ where k , ω and t are the x -directional wavenumber, angular frequency and time. The Christoffel equation^[1] can be written as

$$\begin{bmatrix} C_{11}k^2 - \rho\omega^2 & C_{16}k^2 \\ C_{16}k^2 & C_{66}k^2 - \rho\omega^2 \end{bmatrix} \begin{Bmatrix} u_x \\ u_y \end{Bmatrix} = 0, \quad (1)$$

Non-trivial solutions for Eq. **Erreur ! Source du renvoi introuvable.** can be found if $k = \pm\alpha$ or $k = \pm\beta$ where

$$\alpha = \sqrt{\frac{\rho\omega^2 (C_{11} + C_{66}) - \rho\omega^2 \sqrt{(C_{11} - C_{66})^2 + 4C_{16}^2}}{2(C_{11}C_{66} - C_{16}^2)}}, \quad (2)$$

$$\beta = \sqrt{\frac{\rho\omega^2 (C_{11} + C_{66}) + \rho\omega^2 \sqrt{(C_{11} - C_{66})^2 + 4C_{16}^2}}{2(C_{11}C_{66} - C_{16}^2)}}.$$

Therefore, the general solution in the anisotropic slab can be expressed as

$$\begin{aligned} u_x &= (AP_x e^{j\alpha x} + BP_x e^{-j\alpha x} + CQ_x e^{j\beta x} + DQ_x e^{-j\beta x}) e^{-j\omega t}, \\ u_y &= (AP_y e^{j\alpha x} + BP_y e^{-j\alpha x} + CQ_y e^{j\beta x} + DQ_y e^{-j\beta x}) e^{-j\omega t}. \end{aligned} \quad (3)$$

The symbols A and B denote unknown amplitudes corresponding to $k = +\alpha$ and $k = -\alpha$, respectively. Likewise, C and D are unknown amplitudes corresponding to $k = +\beta$ and $k = -\beta$, respectively.

From Eq. **Erreur ! Source du renvoi introuvable.**, the displacement components corresponding to the α and β waves can be expressed as

$$\begin{aligned} u_x^\alpha &= (Ae^{j\alpha x} + Be^{-j\alpha x})P_x e^{j\omega t}, u_y^\alpha = (Ae^{j\alpha x} + Be^{-j\alpha x})P_y e^{j\omega t}, \\ u_x^\beta &= (Ce^{j\beta x} + De^{-j\beta x})Q_x e^{j\omega t}, u_y^\beta = (Ce^{j\beta x} + De^{-j\beta x})Q_y e^{j\omega t}, \end{aligned} \quad (4)$$

where $P_x, P_y, Q_x,$ and Q_y represent the polarization vector components. They are found to be

$$P_x = \frac{X_\alpha}{\sqrt{1+|X_\alpha|^2}}, P_y = \frac{1}{\sqrt{1+|X_\alpha|^2}}, Q_x = \frac{X_\beta}{\sqrt{1+|X_\beta|^2}}, Q_y = \frac{1}{\sqrt{1+|X_\beta|^2}}, \quad (5)$$

where

$$X_k = -\frac{C_{16}k^2}{C_{11}k^2 - \rho\omega^2} = -\frac{C_{66}k^2 - \rho\omega^2}{C_{16}k^2} \quad (k = \pm\alpha, \pm\beta). \quad (6)$$

The symbol X_k represents the amplitude ratio of u_x and u_y . Due to the orthogonality of the wave mode, the relation that $P_x Q_x + P_y Q_y = 0$ always holds.

One can express the velocity (v_x and v_y) and stress (σ_{xx} and σ_{xy}) as

$$\begin{Bmatrix} v_x \\ v_y \\ \sigma_{xx} \\ \sigma_{xy} \end{Bmatrix}_{x=d} = \mathbf{MN} \begin{Bmatrix} A \\ B \\ C \\ D \end{Bmatrix}. \quad (7)$$

Please see Appendix for the elements of the \mathbf{M} and \mathbf{N} matrices. If C_{ij} and ρ are replaced by c_{ij} and ρ_0 in the equations above, the corresponding results are applicable for the base medium. In this case, the x -directional wave numbers will be denoted α_0 and β_0 .

2.2 Transmissions and reflections

To obtain the scattering (\mathbf{S}) parameters, we first write the relationship between the velocity and stress fields on the left and the right boundaries of the anisotropic slab (see Figure. 1a of the main text),

$$\begin{Bmatrix} v_x \\ v_y \\ \sigma_{xx} \\ \sigma_{xy} \end{Bmatrix}_{x=d^-} = \mathbf{MN}_{x=d} \mathbf{M}^{-1} \begin{Bmatrix} v_x \\ v_y \\ \sigma_{xx} \\ \sigma_{xy} \end{Bmatrix}_{x=0^+} = \mathbf{T}_{x=d} \begin{Bmatrix} v_x \\ v_y \\ \sigma_{xx} \\ \sigma_{xy} \end{Bmatrix}_{x=0^+}. \quad (8)$$

By imposing the continuities between the field variables of the base medium and those of the anisotropic slab at $x=0$ and $x=d$, we can obtain the \mathbf{S} matrix as

$$\mathbf{S} = \mathbf{M}_0^{-1} \mathbf{T}_{x=d} \mathbf{M}_0, \quad (9)$$

where \mathbf{M}_0 is the \mathbf{M} matrix for the base medium. The \mathbf{S} matrix represents the relationship between the displacement amplitudes of the adjacent base medium at $x=0^-$ and those at $x=d^+$.

Once the components (S_{ij}) of the \mathbf{S} matrix are determined, the reflection and transmission coefficients for the case of longitudinal wave incidence can be expressed as:

$$\begin{aligned} RLL &= \frac{S_{24}S_{41} - S_{44}S_{21}}{S_{22}S_{44} - S_{42}S_{24}}, \\ RLT &= \frac{S_{42}S_{21} - S_{22}S_{41}}{S_{22}S_{44} - S_{42}S_{24}}, \\ TLL &= S_{11} + S_{12}RLL + S_{14}RLT, \\ TLT &= S_{31} + S_{32}RLL + S_{34}RLT. \end{aligned} \quad (10)$$

In Eq. **Erreur ! Source du renvoi introuvable.**, RLL and RLT denote the reflection coefficients for the reflected L and T waves, respectively, and TLL and TLT , the transmission coefficients for transmitted L and T waves, respectively. The explicit expressions for the elements of the \mathbf{T} and \mathbf{S} matrices are given in Appendix.

The mode conversion ratio, i.e. the L-to-T transmission power ratio (T_T) represents the ratio of the transmitted S-wave power intensity (P^{TLT}) to the incident L-wave power intensity (P^L). Therefore, it can be expressed as

$$T_T = \frac{P^{TLT}}{P^I} = \frac{\text{real}\left(\sigma_{xy}^{TLT} \times \text{conj}\left(v_y^{TLT}\right)\right)\big|_{x=d^+}}{\text{real}\left(\sigma_{xx}^I \times \text{conj}\left(v_x^I\right)\right)\big|_{x=0^-}} = \xi |TLL|^2, \quad (11)$$

where

$$\xi = \frac{\beta_0 c_{66}}{\alpha_0 c_{11}}. \quad (12)$$

Similarly, the L-to-L transmission power ratio (T_L) representing the ratio of the transmitted T-wave power intensity (P^{TLL}) to the incident L-wave power intensity (P^I) can be obtained as

$$T_L = \frac{P^{TLL}}{P^I} = \frac{\text{real}\left(\sigma_{xx}^{TLL} \times \text{conj}\left(v_x^{TLL}\right)\right)\big|_{x=d^+}}{\text{real}\left(\sigma_{xx}^I \times \text{conj}\left(v_x^I\right)\right)\big|_{x=0^-}} = |TLL|^2. \quad (13)$$

The reflections of the L wave and T wave can be written as

$$R_L = |RLL|^2, R_T = \xi |RLT|^2. \quad (14)$$

2.3 Theory for Full mode-converting transmission

Here, we mainly consider the bimodal quarter-wave impedance matching theory^[10], which allows full mode-converting transmission. In this theory, four necessary conditions are needed:

1) Bimodal quarter-wave phase matching condition:

$$d = n_{FS} \frac{\lambda_{FS}}{4}, \quad (15a)$$

$$d = n_{SS} \frac{\lambda_{SS}}{4}, \quad (15b)$$

$$\frac{n_{SS}}{2} - \frac{n_{FS}}{2} = \text{odd}, \quad (15c)$$

where n_{FS} and n_{SS} are integers. These conditions are equivalent to $\sin(\alpha d) = \pm 1$ and $\sin(\beta d) = \mp 1$.

2) Bimodal impedance matching condition:

$$\tilde{Z} = \tilde{Z}_0, \quad (16)$$

where $\tilde{Z} = \sqrt{\frac{\gamma}{\rho} - C_{16}^2}$ and $\tilde{Z}_0 = \sqrt{\frac{\gamma}{\rho} - c_{66}^2}$ denote the bimodal impedances of the anisotropic metamaterial and background isotropic medium, respectively.

3) Polarization condition:

$$C_{11} = C_{66}, \quad (17)$$

which implies that the fast skew and slow skew modes have $\pm 45^\circ$ polarizations, respectively.

4) Weak mode-coupling condition:

$$\varepsilon = C_{16} / C_{11} \rightarrow 0. \quad (18)$$

With the above four conditions, one can find that at the bimodal quarter-wave phase matching frequency,

$$\lim_{\varepsilon \rightarrow 0} R_L(f_{BQW}) = 0, \lim_{\varepsilon \rightarrow 0} R_T(f_{BQW}) = 0, \lim_{\varepsilon \rightarrow 0} T_L(f_{BQW}) = 0, \lim_{\varepsilon \rightarrow 0} T_T(f_{BQW}) = 1. \quad (19)$$

The anisotropic slab must have specific anisotropy, which can be described as follows,

$$C_{11} = C_{66} = \frac{\tilde{Z}_0}{2\rho} \left(\frac{\gamma_{SS}}{n_{FS}} + \frac{n_{FS}}{n_{SS}} \right) \quad (20a)$$

$$C_{16} = \frac{\tilde{Z}_0}{2\rho} \left(\frac{\gamma_{SS}}{n_{FS}} - \frac{n_{FS}}{n_{SS}} \right), \quad (20b)$$

$$\rho = \frac{\sqrt{\tilde{\epsilon}_{U_{rs}}}}{4f_{BQW}d}. \quad (20c)$$

3. DESIGN WITH RESONANCE MECHANISM

In this work, we consider to introduce the resonance mechanism by designing anisotropic metamaterials in the short wavelength limit. Because the target wavelength could be much larger than the unit cell dimension, resonance could naturally occur. Based on this idea, we aim to design the bimodal quarter-wave impedance matching element by cutting slits on an aluminum plate.

Figure 1 shows the designed metamaterial, which is obtained by cutting two columns of slits on the aluminum matrix. As for its geometric information, $h=2\text{cm}$, $w=3\text{cm}$, $l=0.18\text{cm}$, $r=1.8\text{mm}$, $\theta=31^\circ$.

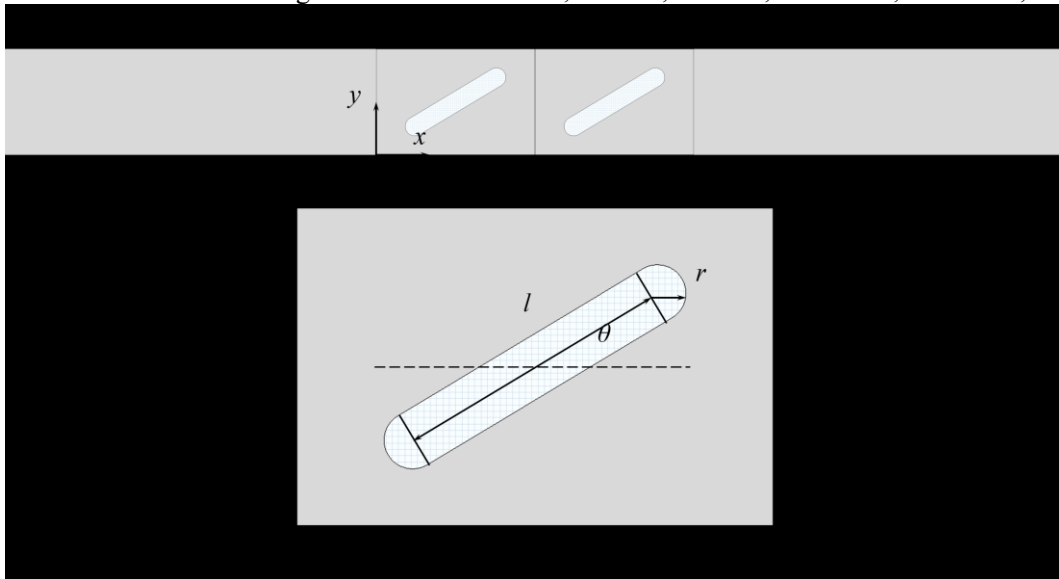


Figure 1 Designed anisotropic metamaterial

Its mode-converting performance is plotted in Figure 2, which shows that the mode-converting efficiency reaches as high as 75% around $f=150\text{kHz}$.

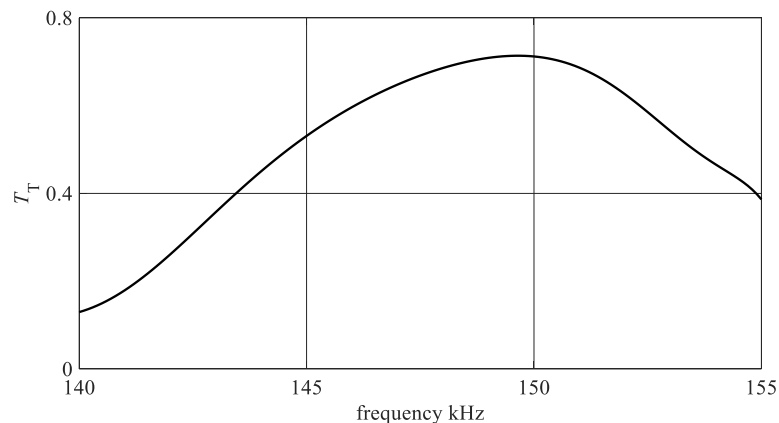


Figure 2 Mode conversion efficiency

Although efforts are still needed to improve the mode-converting efficiency, one may still see the potentials in designing anisotropic metamaterials by introducing resonance mechanism. Firstly, if the anisotropic metamaterial were design in the long wavelength limit, on the other hand, it would behave as a nonresonant composite. It can then be noticed that the bimodal impedance matching condition in Eq. (16) can never be satisfied by cutting silts on a matrix. However, the satisfaction could be possible in the short wavelength limit, because the metamaterial can have frequency-dependent effective material properties.

Secondly, if subwavelength unit cell means that the microstructure should be much smaller than

the wavelength. This would make the actual fabrication very difficult, not to mention that much more unit cells need to be fabricated. In this design case, the minimum feature of the unit cell is $r=1.8\text{mm}$, which is very easy for fabrication, and only two layers need to be machined. This could significantly broaden the application of elastic metamaterials, especially in ultrasonic ranges.

Because a dynamic homogenization method needs to be developed to reveal the intrinsic influence of the resonance mechanism through evaluating the effective properties of the metamaterial, the actual evaluation of the effective properties will not be discussed here.

4. SUMMARY

In this work, we have a brief discussion on designing metamaterials in short wavelength range. Because working in the short wavelength range means the resonance could occur, effective material properties of the metamaterials could exert much more possibilities in satisfying strict material requirements for extraordinary wave phenomena. Motivated by this observation, we tried to realize an efficient mode-converting efficiency through cutting two columns of slits on an elastic matrix. With this simple design, the mode-converting efficiency reached over 70%.

ACKNOWLEDGEMENTS

The authors sincerely acknowledge the financial support from the National Natural Science Foundation of China (11802220, 11772251), the Natural Science Basic Research Plan in Shaanxi Province of China (2019JQ-293), and the 111 Project (B18040).

REFERENCES

1. Zhang J, Drinkwater BW, Wilcox PD, Hunter AJ. Defect detection using ultrasonic arrays: The multi-mode total focusing method. *NDT & E International* 2010; 43(2):123-133.
2. Tufail Y, Yoshihiro A, Pati S, Li MM, Tyler WJ. Ultrasonic neuromodulation by brain stimulation with transcranial ultrasound. *Nat. Protoc.* 2011; 6:1453-1470.
3. Clement GT, White PJ, Hynynen K. Enhanced ultrasound transmission through the human skull using shear mode conversion. *J. Acoust. Soc. Am.* 2004; 115(3): 1356-1364.
4. B. A. Auld, *Acoustic Fields and Waves in Solids*, Krieger Publishing Company, Malabar, FL; 1990.
5. Wu Y, Lai Y, Zhang ZQ. Elastic Metamaterials with Simultaneously Negative Effective Shear Modulus and Mass Density. *Phys. Rev. Lett.* 2011; 107: 105506.
6. Zhu R, Liu XN, Hu GK, Sun CT, Huang GL. Negative refraction of elastic waves at the deep-subwavelength scale in a single-phase metamaterial. *Nat. Commun.* 2014; 5: 5510.
7. Zhu R, Liu XN, Huang GL. Study of anomalous wave propagation and reflection in semi-infinite elastic metamaterials. *Wave Motion* 2015; 55: 73-83.
8. Kweun JM, Lee HJ, Oh JH, Seung HM, Kim YY. Transmodal Fabry-Perot resonance: theory and realization with elastic metamaterials. *Phys. Rev. Lett.* 2017; 118: 205901.
9. Yang XW, Kweun JM, Kim YY. Theory for perfect transmodal Fabry-Perot interferometer. *Sci. Rep.* 2018; 8: 69.
10. Yang XW, Kim YY. Asymptotic theory of bimodal quarter-wave impedance matching for full mode-converting transmission. *Phys. Rev. B* 2018; 98: 144110.